AIIM

Association for Information and Image Management

1100 Wayne Avenue, Suite 1100
Silver Spring, Maryland 20910

301/587-8202

Centimeter

Inches

COMBUSTION BEHAVIOR OF SINGLE COAL-WATER SLURRY DROPLETS. PART I: EXPERIMENTAL TECHNIQUES

Yiannis A. Levendis
Mohamad Metghalchi and Don Wise
Department of Mechanical Engineering
Northeastern University
Boston, MA. 02115

Abstract

Techniques to produce single droplets of coal-water slurries have been developed in order to study the combustion behavior of the slurries. All stages of slurry combustion are of interest to the present study, however, emphasis will be given to the combustion of the solid agglomerate char which remains upon the termination of the water evaporation and the devolatilization periods. An experimental facility is under construction where combustion of coal-water slurries will be monitored in a variety of furnace temperatures and oxidizing atmospheres. The effect of the initial size of the slurry droplet and the solids loading (coal to water ratio) will be investigated. A drop tube, laminar flow furnace coupled to a near-infrared, ratio pyrometer will be used to monitor temperature-time histories of single particles from ignition to extinction. This paper describes the experimental built-up to this date and presents results obtained by numerical analysis that help understanding the convective and radiating environment in the furnace.

INTRODUCTION

The use of coal-water slurries (CWS) as a substitute for oil as an energy source is economically and politically attractive as it reduces dependence on imported petroleum. It has been suggested that coal-water slurries can replace oil in many applications with only an approximate 3.5% loss in heat energy[1]. This alternate technology for coal utilization consists of mixing finely crushed coal in water and then burning the mix in retrofitted stationary power plants, industrial boilers or even turbines and diesel engines. Additional beneficial features of such slurries include their pumpability that enables transportation of coal in pipe-lines over long distances, their ease of handling, and good furnace feeding characteristics. Although many advantages derive from the use of coal-water slurries the large quantity of the associated water can impair flame ignition and stability with detrimental effects on combustion efficiency and pollutant formation.

Fundamental research by Law and coworkers[1,2,3] and Szekely and Faeth[4,5,6] involving oxidation of single coal-water drops in the post combustion region of a flat flame burner revealed that the combustion process takes place in four different stages. The first stage involves evaporation of water, the second the heat-up and pyrolysis of coal particle agglomerates, the third the evolution and gas-phase combustion of volatiles, and the fourth the heterogeneous combustion of the remaining char. The last step was observed to be the slowest requiring up to 90-95% of the droplet life time[6] and, therefore, it will be the controlling step during spray combustion in a practical combustion chamber. These char agglomerates were also observed to extinguish and remain unburned in regions of the combustor where the equivalence ratio significantly deviated from stoichiometry[6]. Use of a lead compound catalyst considerably extended the flamability limits in the lean mixture region[6].

The various stages of coal-slurry combustion have been studied by several investigators. Tran *et al.*[7] have concentrated their studies in the processes that take place during the evaporation of water from the CWS droplet. Using intense laser heating in an electrodynamic balance they concluded that the presence of the suspension agents (surfactants) in the slurries were impeding the evaporation process. Since water may induce microexplosion and intensify fragmentation of the agglomerates[6] upon rapid heating the above experiments were conducted below the explosive boiling limit. Zghoul and Essenhigh[8] observed that heat-up, evaporation and ignition times for CWS were proportional to the first power of the initial droplet diameter. The combustion of the devolatilized char residue (fourth stage) has been modeled in the manner of a burning carbon sphere[1,5,6] since it was determined that the coal burns in the form of agglomerates rather than individual particles. Incidentally, the mechanism that binds the coal particles and holds them together in one agglomerate is not well understood. Dunn-Runkin et al.[9] suggested explanations involving the thermoplasticity of coal and/or monolayers of water between the particles that serve as the glue in the coal-water agglomerates, however, the latter may not apply to high temperature pyrolysis[9]. Other investigators[9-14] have examined the effects of various parameters like the droplet size, coal mass fraction and coal type on the evaporation and combustion of slurry droplets. Others[15-17] have undertaken studies of the mechanisms of coal water atomization and spray formation.

Although numerous experimental and theoretical studies have been reported in the literature and a good foundation for understanding slurry droplet combustion exists there are still serious limitations, technical problems and uncertainties. Many experimental studies have dealt with combustion of large drops (around 1000μm) which, however, are not of interest to typical combustion feed streams or have not adequately addressed the region of high temperatures (above 1500 K) encountered in practical applications. Furthermore derivation of intrinsic chemical kinetics taking into account the developing pore structure during the particle combustion history has not been considered.

The present investigation aims at furthering our understanding of the combustion behavior of coal water slurries by isolating drops of size of interest to combustion in utility boilers (50-200μm). The burnout history of the coal particle is going to be recorded and the particle temperature will be measured in the manner of Levendis and Flagan[18,19] for solid and cenospheric particles. This technique, coupled to physical characterization of captured chars will facilitate derivation of reaction rates.

EXPERIMENTAL

Micronized and beneficiated slurries provided by *Otisca* are used in this study. To keep the slurries from sedimenting an apparatus was constructed to continuously tumble bottles of slurry at slow speed using a small motor, Fig. 1.

Laminar Furnace Construction

The furnace is a drop tube, laminar flow device manufactured by *ATS*, utilizing *Kanthal Super 33* molybdenum disilicide heating elements, to heat a 25 cm long radiation cavity to temperatures up to 1650 °C.

A 60 cm long 7 cm i.d. high purity alumina tube, manufactured by *Coors*, has been installed along the centerline of the furnace as shown in Fig. 1. The furnace is also equipped with two diagonally opposite side observation windows which are fitted with quartz glass and a shutter. The vertical alumina tube is supported at the upper and lower end by water cooled, stainless steel "O-ring" assemblies which also provide for an air tight system, Fig. 1. The top utilizes a *Viton* "O-ring", meanwhile the bottom employes alumina insulation blanket in the form of a ring compressed in the assembly in order to withstand the high temperatures.

A movable, stainless steel, water cooled injector was positioned at the top of the drop tube furnace, designed to to perform a dual function: (**a**) enable injection of particles or drops at various heights in the furnace radiation cavity, and (**b**) enable pyrometric observations of burning particles from the top of the furnace. For the latter purpose the injector should be: on one hand short and wide to maximize collection of light emitted from burning particles ($I_{rad} \propto (distance)^{-2}$), and on the other hand long and narrow to avoid observation of *direct* radiation from the furnace walls. The final design, 57 cm long and 1 cm i.d., was a compromise of the above two criteria. Then the injector was passivated black to minimize *reflected* furnace-wall radiation from climbing up to the top where the light collecting optics are situated. A brass flange supports the injector through a *Cajon* fitting, and provides for the introduction of the main furnace air through a metallic screen that serves as a flow straightener.

A second narrow passage, air flow straightener was machined out of low density alumina material, and placed in the annular space between the injector and the tubular furnace wall to break small eddie vorticity, Fig. 1.

Furnace air flows are regulated by a *Matheson* electronic mass flow meter (1-20 lpm), and needle-valve *Matheson* rotameter (0.01-1.0 lpm). Rotameters are also used to regulate mixing of nitrogen and oxygen gases to control the composition of the oxidizing gas in experiments where oxygen concentrations other than 21% (air) are required.

Suction Thermometry

While furnace wall temperatures were monitored by type *B* thermocouples attached to the wall, gas temperatures inside the furnace were measured by a suction thermometer, shown in Fig. 2. This instrument utilized a type S thermocouple in a sheath inside a 0.9 cm i.d., 57 cm long, high density alumina tube. The thermocouple junction was placed at a distance of 2 cm from the top end. The bottom end of the alumina tube was attached to a pump to provide suction. Low density alumina blanket was inserted between the thermocouple sheath and the tube to serve as a radiation shield for the thermocouple tip. The pump suction drove furnace gases around the thermocouple junction through the permeable blanket in order to lower the blanket temperature to the gas temperature. The flowrate was increased till the temperature, recorded by the thermocouple, reached a minimum value asymptotically. This closely corresponds to the gas temperature. To ensure that the flow profile inside the furnace was disturbed minimally, sampling was performed isokineticaly by adjusting the inlet cross sectional area of the suction thermometer. Two sets of gas temperature data are shown in Fig. 3. It can be seen that, at the flow conditions where most experiments are expected to take place, the gas temperature is fairly constant in the radiation cavity except under high injector velocities where the injector jet momentum dissipation is slow, as explained in the next section. Average gas temperatures are measured to be about 60 K lower than the wall temperatures.

Optical Pyrometry

A three color pyrometer has been constructed and is almost ready for particle radiation monitoring. The pyrometer employes a state of the art, 1 mm diameter thick, 1.6 m long, single optical fiber, manufactured by *General Fiber Optic*, to transmit light from the collimator-pinhole system that is situated at the top of the furnace injector. Details of this arrangement are shown in Fig. 4. At the pyrometer end of the optical fiber an other collimator is employed to guide the light to two consecutive beam splitters. The three resulting light beams are directed through narrow bandwidth (10 nm) interference filters and focussing optics to solid state detectors. The three filters employed have wavebands centered at 800, 975 and 1200 nm. To optimize the detection effectiveness at these wavelengths the first two filters are coupled to silicon detectors, meanwhile the last one to a germanium detector.

The output of linear pre-amplification circuits is conducted to logarithmic amplification circuits to provide ample amplification over a large range of particle temperatures.

Production of Single Drops

Techniques to produce single droplets of coal-water slurries are been developed in order to study the combustion behavior of the slurries. Two different types of droplet generators are under investigation: **(i)** one that utilizes mechanical means i.e. the action of a plunger to push a small quantity of slurry out of an orifice, and **(ii)** a generator that utilizes electrically driven piezoelectric transducers to generate a pressure wave and create a drop. We have assembled a working design of the former category shown in Fig. 4. The core element is supplied by *Xandex* and consists of a small cavity with a needle attached at the bottom. A thin plastic plunger is mounted at the centerline of the cavity and runs through the needle all the way to the bottom tip. Lifting the plunger, by spring motion from the top, slurry flows around the plunger to the space between the tip of the needle and the end of the plunger. Then application of a sudden force (impact) to the plunger expels a drop, Fig. 5. The size of the drops can be controlled by various diameters of needle-plunger combinations. The technique is fairly repeatable and only the smallest needles used experience frequent plugging problems. Photographs of generated drops are shown in Fig. 5. Drop size is 700μm, and 400μm in Figs. 5a and 5b, respectively.

Designs of the electrically driven generators use the principle of the uniform break-up of a liquid jet when a periodic disturbance is imposed. To drive these drop generators a single pulse electrical signal generator has been constructed. This device is capable of creating pulses having durations in the range of 1 ms to 1 sec, and amplitudes up to 30 V. The dimensions of the piezoelectric elements are calculated based on the required volume displacement. The design criteria are:

- Ease of construction - making electrical connections and connecting the transducer to the reservoir and capillary tube.
- Ease of use - filling with coal water slurries without air bubbles in the system, emptying and cleaning.
- Effectiveness of transmission of the motion of the transducer to the fluid. This is important in order to maximize the amplitude of the pressure wave and volume displacement.
- Effectiveness with which the primary pressure wave is transmitted to the orifice - in other words eliminate as far as possible restrictions and obstructions which could dissipate the energy in the wave, and provide a smooth flow path from the transducer to the orifice.

Two different designs are been built, one using a stack of transducers connected in series and the other using a bimorph epoxied on a metallic membrane. Both designs are coupled to extruded glass orifices. No results have been obtained yet.

Finally, to gain understanding of the physical transformations that take place during combustion of char agglomerates, partially burned agglomerates will be removed from the furnace by means of a water-cooled collector probe. Such a probe has been constructed and utilizes nitrogen to facilitate "freezing" the combustion reactions.

FLUID FLOW MODELLING

Combustion experiments will be carried out in the experimental apparatus described above, the laminar flow, drop tube furnace. Despite the fact that the thermal and flow environment of this furnace is much more well characterized than any real life turbulent coal burner it still presents considerable challenge to account for it. Even if the temperature of the furnace walls in the radiation cavity has been measured to be relatively uniform burning particles will also see the injector opening and walls, the second flow straightener, the furnace walls above and below the radiation cavity, and the exit opening or the collection probe at the bottom of the furnace. The view factor to all of these furnace parts will depend on the vertical position (and the radial position) in the furnace where the particle ignites as well as the velocity profiles in the furnace. The gas temperature that the particle burns at is also varying during burntime and is a function of both the injector and furnace gas flowrates. To model the velocity and temperature environment in this furnace the *Fluent* software package, developed by *Creare* (1989) was utilized. Thus, numerical solutions for the gas phase can be obtained by simultaneously solving the continuity, momentum and energy equations. Of particular interest is the gas phase environment near the tip of the particle injector where steep velocity and gas temperature gradients are expected. The program can be used to study the effects of the injector and furnace flow rates, as well as the importance of the vertical position of the injector and the flow straightener. Furthermore an other feature of this program can handle the introduction of a second phase i.e. a liquid drop or a solid particle. Thence, the trajectory of the drop can be studied, and the time for vaporization and remaining solid heat-up can be estimated.

Results obtained with Fluent for one case are shown in Figs. 6a-c for an injector flow rate of 0.5 lpm, main furnace flow rate of 2 lpm and a furnace wall temperature, T_w, of 1500 K in the radiation cavity. T_w at the regions were the top and bottom insulation sections exist was assumed to decrease according to a linear ramp profile[20]. The entering temperature of air at the second flow straightener was set to 800 K in this case extrapolating from measurements made elsewhere[20]. In all of these plots the scale in the radial direction has been expanded by 2.5 times. Fig. 6a and 6b depict the velocity profiles in the axial and radial direction, respectively. In Fig. 6c temperature profiles are depicted. It can be seen that the effects of the injector air stream are greatly influencing the flow conditions inside the furnace. Under these conditions it takes a length of over 20 injector inner diameters for the momentum of the jet to dissipate. The highest velocities are observed to take place directly after the exit of the injector. It can also be observed that it takes ca. six injector diameters for the entering gas temperature to climb to values close to T_w. Many different cases have been investigated for furnace flowrates varying between 1 to 2 lpm, injector flowrates between 0.0 and 1.0 lpm, at three wall temperatures: 1150, 1500 and 1850 K. Results are plotted on Figs. 7-10. Figures 7 and 8 illustrate the effects of the injector flowrate on the axial velocity and temperature profiles, respectively. For all these cases the calculated average velocities in the furnace were in the range of 5 to 10 cm/s. Low injector flow rates result in local centerline velocities that do not deviate much from the average velocities, meanwhile injector flowrates of 0.5 to 1.0 result in centerline velocities that are up to 7 times higher than the calculated average. This was a rather unexpected result. Similar trends are noticed in the temperature profiles (Fig. 8). This suggests that the injector flowrates should be kept to the neighborhood of 0.1 lpm if fairly uniform velocity and gas temperature profiles are desired under these conditions.

The effects of the furnace flowrate on the centerline temperature were minimal as shown in Fig. 9. The effects of the axial position of the flow straightener were also found to be unimportant and moving the flow straightener closer to the injector tip did not seem to influence either the velocity or the temperature profiles in the furnace.

The effect of the wall temperature is shown in Fig. 10 where the difference between the furnace mean wall temperature, MWT, and the centerline temperature T_c is plotted for the case of an injector flow rate of 0.5 lpm. The largest temperature gradients are experienced at the highest wall temperatures and it takes six injector diameters for the centerline to heat to within 200 K from the wall temperature. The corresponding distance for the case of an injector flow rate of 0.1 lpm is one injector diameter only , Fig. 8.

The fate of introduced water droplets in the furnace environment can also be modelled with the *Fluent* software package. The results are shown in Figs. 11a and 11b as two symmetric particle trajectories. In both cases the injector and furnace flowrates were set at 0.1 and 2.0 lpm, respectively and the wall temperature at 1500 K. Entering particle velocities were were set equal to terminal velocities by equating the aerodynamic drag forces equal to the gravity forces. Figure 11a shows the fate of a 50μm particle, which is seen to evaporate in 0.86 sec inside the water cooled injector. Figure 11b shows the lifetime of a 250 μm water drop which reached the radiation cavity and took an overall of 0.32 sec to evaporate. These results will be verified by an algorithm currently developed.

SUMMARY

Hardware for injection of single coal-water slurry drops in a high temperature environment has been developed. A high temperature, laminar flow furnace has been interfaced with instrumentation capable of monitoring gas and solid particle temperatures inside the radiation cavity as well as total particle burnout times. Numerical techniques are used to model the furnace environment, and optimize injection parameters and gas flow rates. Gas velocity and temperature profiles as well as particle water-evaporation times are also computed.

LITERATURE REFERENCES

1. Liu, G. E. and Law, C. K., *Fuel* **65**, 171, 1986.

2. Miyasaka, K. and Law, C. K. *Combust. Sci. Technol.* **24**, 71, 1980.

3. Szekely, G. A. and Faeth, G. M. *AIAA Jou.* **20**, 422, 1982.

4. Szekely, G. A. and Faeth G. M. in *Nineteenth Symposium (International) on Combustion*, Combustion Institute, Pittsburgh, p.1077, 1983.

5. Szekelly, G. A. (1982) PhD Thesis, Pennsylvania State University, and references therein.

6. Tran, X. P., Maloney, D. J. and Spann, J. F. "Evaporation of Coal-Water fuel Droplets Under Intense Heating Conditions." Presented at the Spring meeting of the Western States Section

of the Combustion Institute, Provo, Utah, April 6-7, 1987.

7. Zghoul, A. M. and Essenhigh, R. H. "Ignition and Combustion Characteristics of Captive Drops of CWS." Central/Western State Section. The Combustion Institute, San Antonio, Texas, 1985.

8. Dunn-Rankin, D., Hoornstra, J., Greulich, F. and Holve, D.J. "Coal Rank Influences on Agglomeration, Swelling and Fragmentation of Coal/Water Slurries During Combustion." Presented at the Spring meeting of the Western States Section of the Combustion Institute, Banff, Alberta, April 27-30, 1986.

9. Yao, S.C., and Manwani, P. *Comb. & Flame* **66**, 87, 1986.

10. Yao, S.C. and Liu, L. "Evaporation and Heating of a Single-Suspended Coal-Water Slurry Droplet in Hot Gas Stream" ASME Paper 82-WA/HT-28, Phoenix, Arizona.

11. Yao, S.C., and Liu, L. *Combust. & Flame* **51**, 335, 1983.

12. Antaki, P. *Combust. Sci. Technol.* **46**, 113, 1986.

13. Antaki, P. and Williams F.A. *Combust. Sci. Technol.* **49**, 289, 1986.

14. Meyer, P. and Chigier, N. "Coal-Water Slurry Atomization" Presented at the Spring meeting of the Western States Section of the Combustion Institute, Banff, Alberta, April 27-30, 1986.

15. Allen, J. W., Rennie, A. G., and Welbourne, M. C. "Atomization of Coal Water Mixtures" *Seventh International Symposium on Coal-Slurry Combustion and Technology*, p.392, New Orleans, LA, May 21-24, 1985.

16. Winters, P.J. and Bailey, R.T. "The effect of Fuel Formulation on the Atomization Characteristics of Coal-Water Mixtures." *Seventh International Symposium on Coal-Slurry Combustion and Technology*, p.392, New Orleans, LA, May 21-24, 1985.

17. Levendis, Y. A., and Flagan, R. C. *Combust. Sci. Technol.* **53**, 2-3, 117, 1987.

18. Levendis, Y.A., Flagan, R.C. and Gavalas, G.R. *Combustion and Flame*, **76**, 221, 1989.

19. Levendis, Y.A., Ph.D. Thesis, CALTECH, 1988.

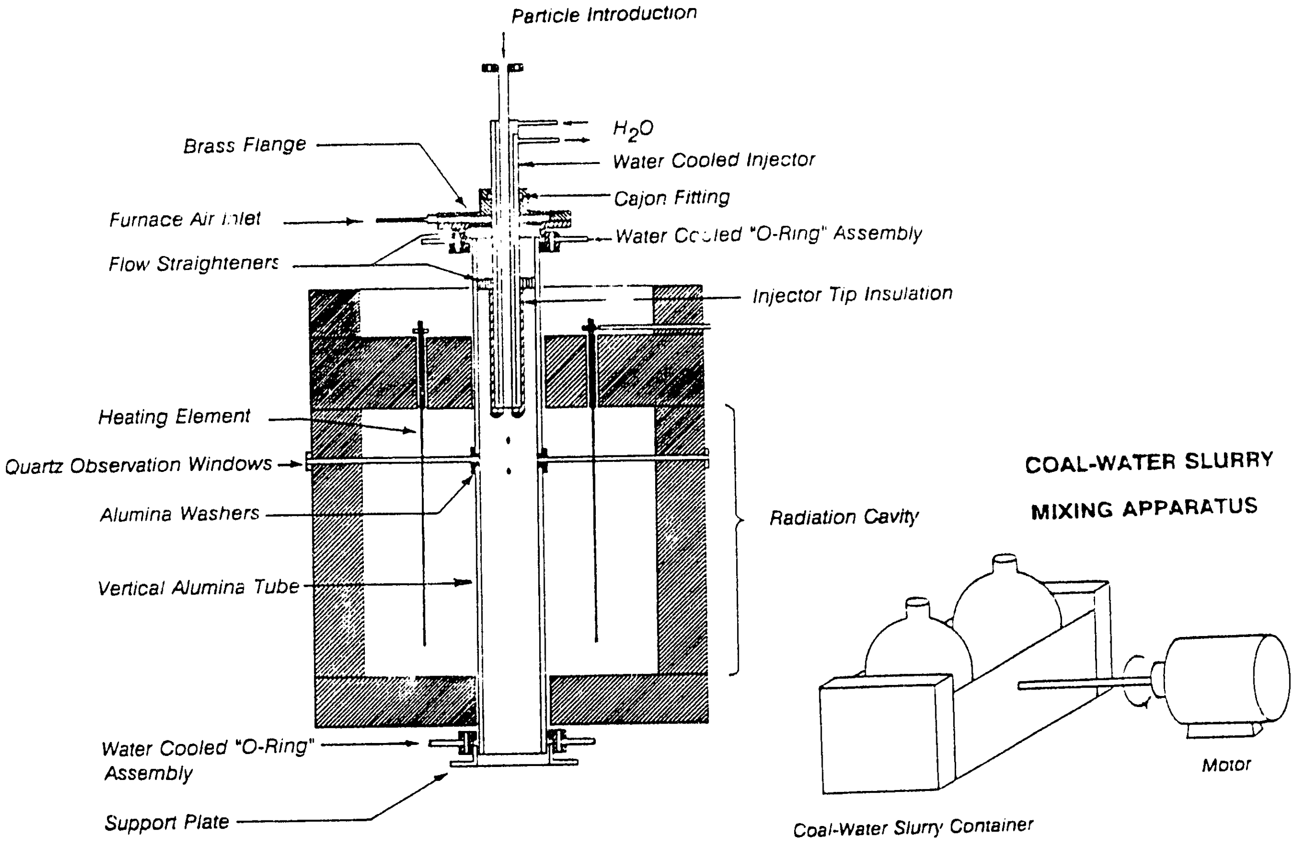

FIGURE 1. Schematic of the laminar, drop-tube furnace and injector assembly. Also shown is the device for the slurry agitator-tumbler.

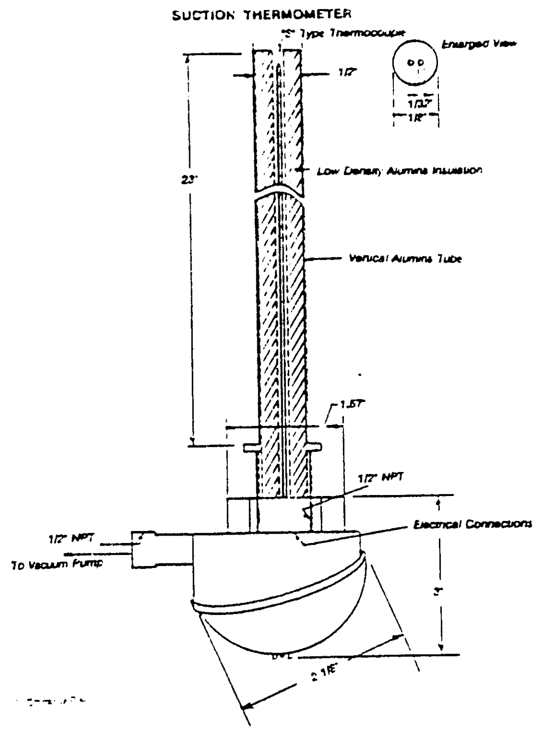

FIGURE 2. Suction Thermometer.

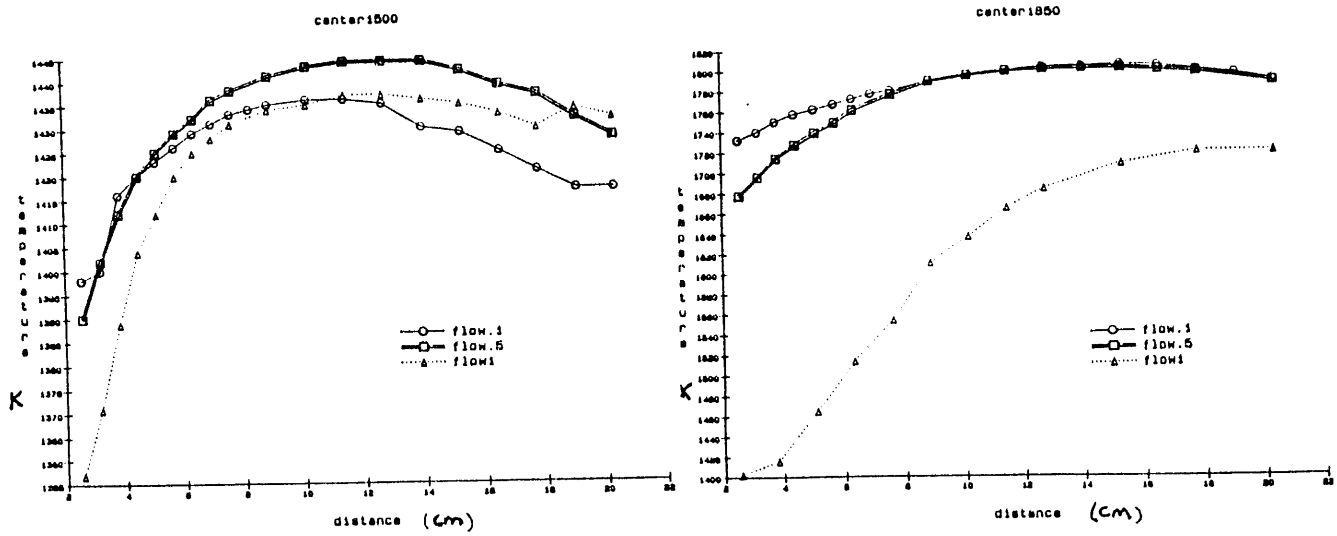

FIGURE 3. Gas temperature profiles along the centerline of the furnace, measured by suction thermometry.

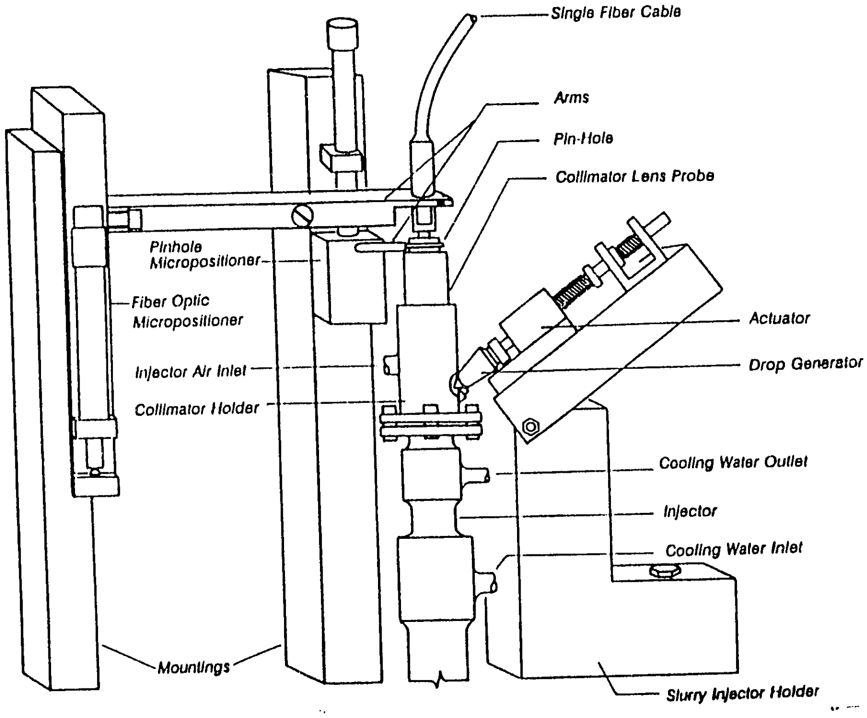

FIGURE 4. Collimating optics-pinhole-fiber optics assembly and the mechanically actuated slurry droplet generator.

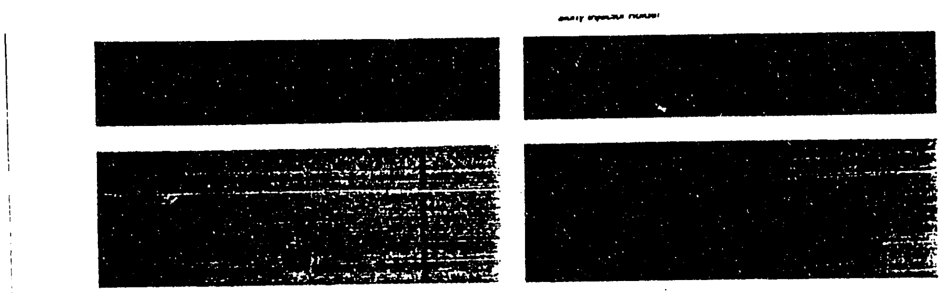

FIGURE 5. Slurry droplet generation with the mechanically actuated generator (a) 700 and (b) 400 μm

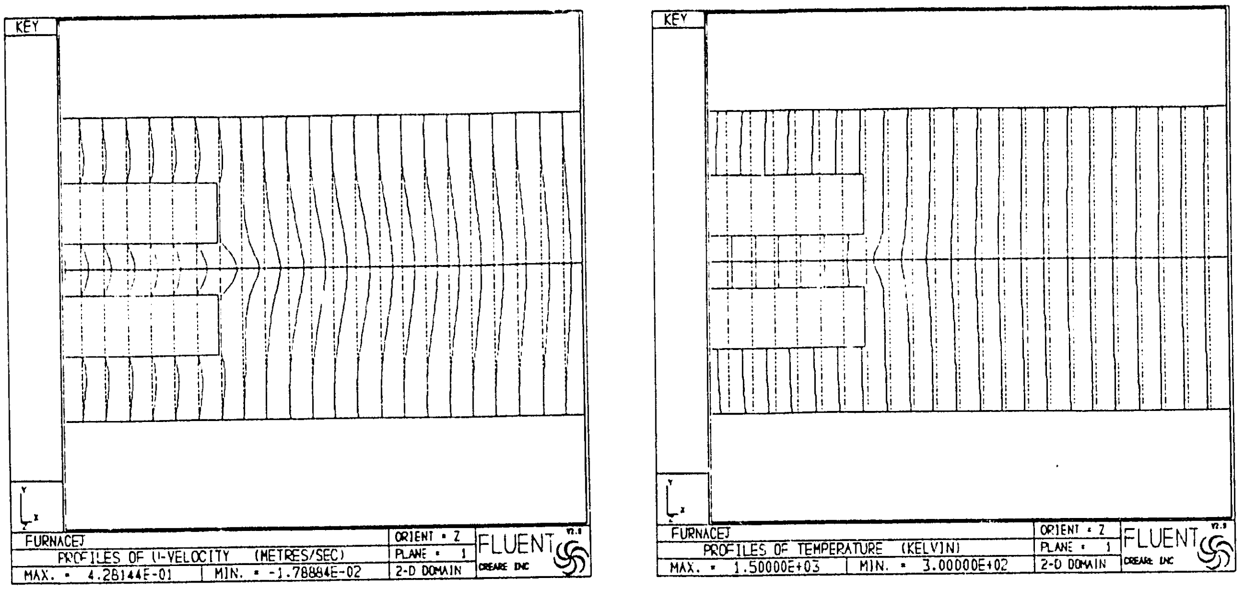

FIGURE 6. Numerical calculations for modelling the air flow inside the drop tube furnace, (i) vertical velocity profiles, (ii) radial velocity profiles, and (iii) temperature profiles. Conditions: furnace air flow-rate 2.0 lpm, injector flow-rate 0.5 lpm and T_w = 1500 K.

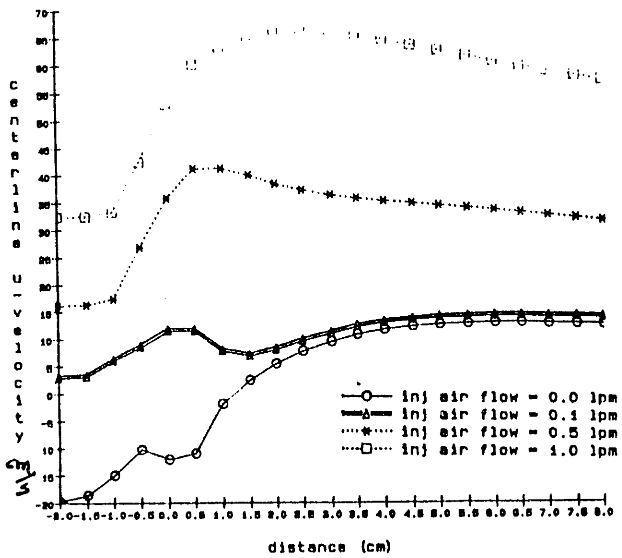

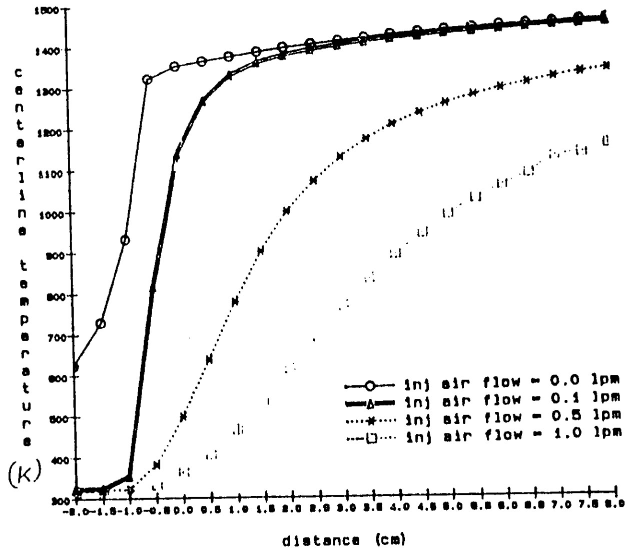

FIGURE 7. Numerical calculations of furnace centerline velocity vs. axial distance from the tip of the injector for four injector flowrates: 0.0, 0.1, 0.5, 1.0 lpm. Furnace flowrate at 2.0 lpm, wall temperature 1500 K.

FIGURE 8. Numerical calculations of furnace centerline temperature vs. axial distance from the tip of the injector for four injector flowrates: 0.0, 0.1, 0.5, 1.0 lpm. Furnace flowrate at 2.0 lpm, wall temperature 1500 K.

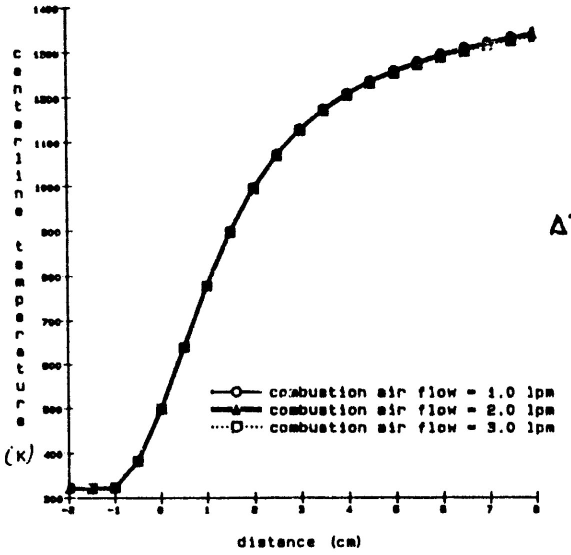

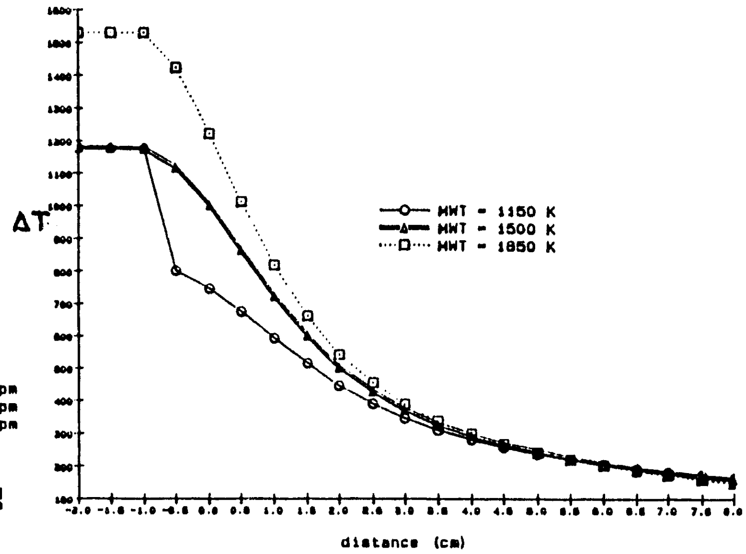

FIGURE 9. Numerical calculations of furnace centerline temperature vs. axial distance from the tip of the injector for three furnace flowrates: 1.0, 2.0, 3.0 lpm. Injector flowrate at 0.5 lpm, wall temperature 1500 K.

FIGURE 10. Numerical calculations of the difference between the maximum furnace wall temperature and the centerline temperature vs. axial distance from the tip of the injector for three wall temperatures 1150, 1500 and 1850 K. Furnace flowrate at 2.0 lpm, and injector flowrate at 0.5 lpm.

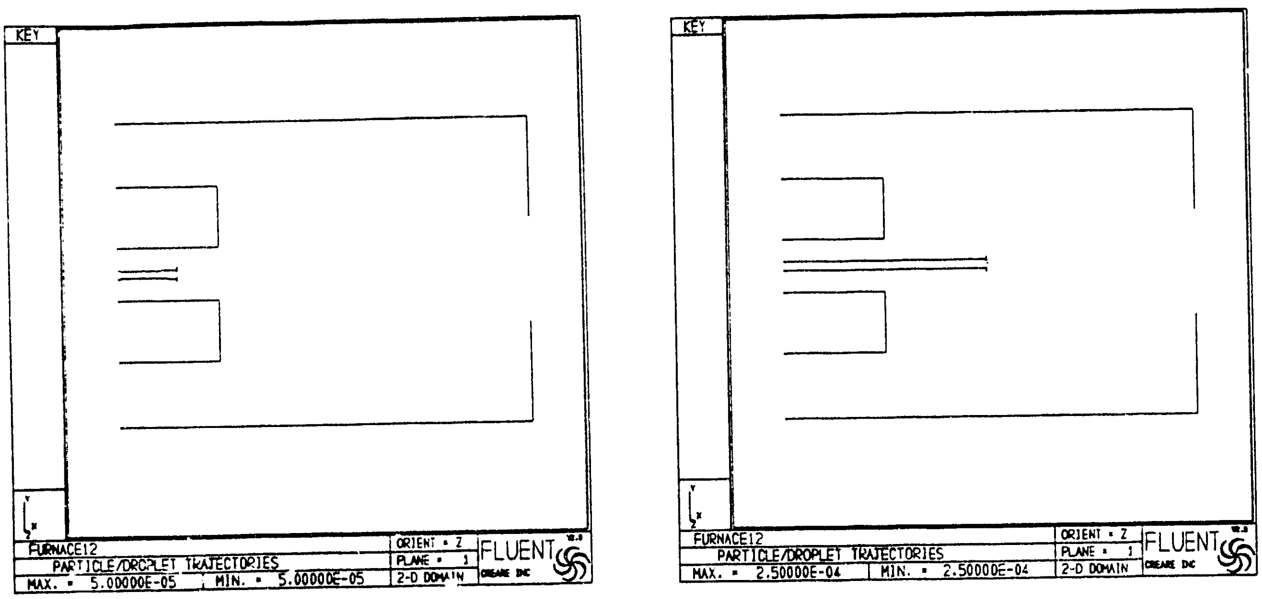

FIGURE 11. Numerical calculations of trajectories of evaporating water drops of 50μm and 250μm water drops. Injector flowrates at 0.1 lpm, furnace flowrate at 2.0 lpm, wall temperature 1500 K.

DATE FILMED

9/23/93

END